

# Syntheses, Characterization, and Magnetic Studies of Copper(II) Complexes with the Ligand *N,N,N',N'*-Tetrakis(2-pyridylmethyl)-1,3-benzenediamine (1,3-tpbd) and its Phenol Derivative 2,6-Bis[bis(2-pyridylmethyl)amino]-*p*-cresol (2,6-Htpcd)

Sabrina Turba,<sup>†</sup> Simon P. Foxon,<sup>†</sup> Alexander Beitat,<sup>†</sup> Frank W. Heinemann,<sup>‡</sup> Konstantin Petukhov,<sup>§</sup> Paul Müller,<sup>§</sup> Olaf Walter,<sup>⊥,∇</sup> Francesc Lloret,<sup>||</sup> Miguel Julve,<sup>\*,||</sup> and Siegfried Schindler<sup>\*,†</sup>

<sup>†</sup>Institut für Anorganische und Analytische Chemie, Justus-Liebig-Universität Gießen, Heinrich-Buff-Ring 58, 35392 Gießen, Germany

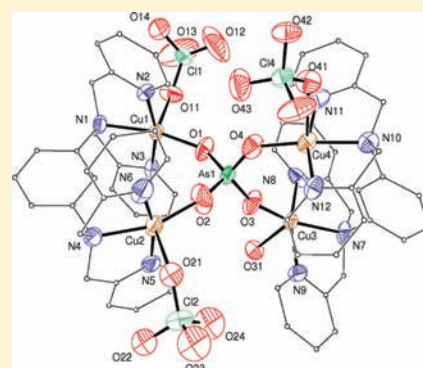
<sup>‡</sup>Institut für Anorganische Chemie, Universität Erlangen-Nürnberg, Egerlandstrasse 1, 91058 Erlangen, Germany

<sup>§</sup>Physikalisches Institut III, Universität Erlangen-Nürnberg, Erwin-Rommel-Strasse 1, 91058 Erlangen, Germany

<sup>⊥</sup>Institut für Technische Chemie—Chemisch-Physikalische Verfahren (ITC-CPV), Forschungszentrum Karlsruhe, Postfach 3640, 76021 Karlsruhe, Germany

<sup>||</sup>Instituto de Ciencia Molecular, Universidad de Valencia, C/ Catedrático José Beltrán 2, 46980 Paterna (Valencia), Spain

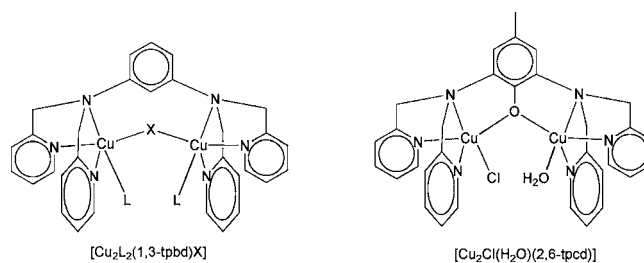
**ABSTRACT:** The copper(II) complexes  $[\text{Cu}_4(1,3\text{-tpbd})_2(\text{H}_2\text{O})_4(\text{NO}_3)_4]_n(\text{NO}_3)_{4n} \cdot 13n\text{H}_2\text{O}$  (**1**),  $[\text{Cu}_4(1,3\text{-tpbd})_2(\text{AsO}_4)(\text{ClO}_4)_3(\text{H}_2\text{O})](\text{ClO}_4)_2 \cdot 2\text{H}_2\text{O} \cdot 0.5\text{SCH}_3\text{OH}$  (**2**),  $[\text{Cu}_4(1,3\text{-tpbd})_2(\text{PO}_4)(\text{ClO}_4)_3(\text{H}_2\text{O})](\text{ClO}_4)_2 \cdot 2\text{H}_2\text{O} \cdot 0.5\text{SCH}_3\text{OH}$  (**3**),  $[\text{Cu}_2(1,3\text{-tpbd})\{(\text{PhO})_2\text{PO}_2\}_2](\text{ClO}_4)_4$  (**4**), and  $[\text{Cu}_2(1,3\text{-tpbd})\{(\text{PhO})\text{PO}_3\}_2(\text{H}_2\text{O})]_{0.69}(\text{CH}_3\text{CN})_{0.31} \cdot 2(\text{BPh}_4)^- \cdot \text{Et}_2\text{O} \cdot \text{CH}_3\text{CN}$  (**5**) [ $1,3\text{-tpbd} = N,N,N',N'$ -tetrakis(2-pyridylmethyl)-1,3-benzenediamine,  $\text{BPh}_4^- = \text{tetraphenylborate}$ ] were prepared and structurally characterized. Analyses of the magnetic data of **2**, **3**, **4**, and  $[\text{Cu}_2(2,6\text{-tpcd})(\text{H}_2\text{O})\text{Cl}](\text{ClO}_4)_2$  (**6**) [ $2,6\text{-tpcd} = 2,6\text{-bis}[\text{bis}(2\text{-pyridylmethyl})\text{amino}]\text{-}p\text{-cresolate}$ ] show the occurrence of weak antiferromagnetic interactions between the copper(II) ions, the bis-terdentate 1,3-tpbd/2,6-tpcd,  $\mu\text{-XO}_4$  ( $\text{X} = \text{As}$  and  $\text{P}$ )  $\mu_{1,2}\text{-OPO}$  and  $\mu\text{-O}_{\text{phenolate}}$  appearing as poor mediators of exchange interactions in this series of compounds. Simple orbital symmetry considerations based on the structural knowledge account for the small magnitude of the magnetic couplings found in these copper(II) compounds.



## INTRODUCTION

Molecular magnetism is an important research field in coordination chemistry. Some highlights on molecular magnets have been summarized previously by Verdaguer and Linert.<sup>1</sup> Inorganic chemists are especially interested in the synthesis of polynuclear transition metal complexes with predictable magnetic properties. Here Kahn and others have provided extensive detailed experimental and theoretical studies in the past to allow some predictions on the magnetic properties of such compounds.<sup>2–12</sup> Blocking ligands and bridging groups play an important role in the synthesis of polynuclear complexes. In our own work we have used tetra-*N*-functionalized 1,3-benzenediamine (*m*-phenylenediamine) as a building block (together with copper(II) ions and coligands) for the formation of polynuclear complexes. Thus, the ligand *N,N,N',N'*-tetrakis(2-pyridylmethyl)-1,3-benzenediamine (1,3-tpbd) and a series of its dinuclear copper(II) complexes (Scheme 1) has been prepared in the past by Schindler and co-workers.<sup>13–17</sup> 1,3-tpbd is a versatile ligand that binds various metal ions in a structurally rigid framework.<sup>14</sup> The phenol-based derivative of 1,3-tpbd, 2,6-bis[bis(2-pyridylmethyl)amino]-*p*-cresol (2,6-Htpcd), once deprotonated, forms dinuclear copper(II) complexes, too (Scheme 1).<sup>14</sup>

**Scheme 1.** (Left) 1,3-tpbd-Bridged Dicopper(II) Complexes with X and L Being Possible Ligands, Where L Can Also Be a Bridging Ligand; (right) Representation of Compound 6 (Charges Are Omitted)



A magnetic study of the structurally characterized perchlorate-bridged dicopper(II) complex  $[\text{Cu}_2(1,3\text{-tpbd})(\text{H}_2\text{O})_2(\text{ClO}_4)_3]\text{ClO}_4$ , with a large intramolecular  $\text{Cu}\cdots\text{Cu}$  separation of 5.873(1) Å, had shown a significant ferromagnetic coupling ( $J = +9.3 \text{ cm}^{-1}$ ,

Received: May 18, 2011

Published: December 6, 2011

the Hamiltonian being defined as  $H = -JS_1 \cdot S_2$ ), which is mediated by the *m*-phenylenediamine unit.<sup>15</sup> Ferromagnetic coupling (parallel spin alignment) is difficult to accomplish because the antiparallel alignment of the local spins (antiferromagnetic coupling) is the most common situation for the magnetic interaction between paramagnetic centers through diamagnetic bridging ligands. Ferromagnetic coupling between copper(II) ions arising from spin polarization effects across polyatomic bridges is rare. Taking into account that the values of the exchange coupling (*J*) were quite large, we became interested to further investigate such compounds. However, more recent results with regard to magnetic properties of complexes with 1,3-tpbd as a bridging ligand were somewhat frustrating. No magnetic coupling was observed when the perchlorate group in  $[\text{Cu}_2(1,3\text{-tpbd})(\text{H}_2\text{O})_2(\text{ClO}_4)_3]\text{ClO}_4$  was replaced by acetate or by sulfate in the tetranuclear complex  $[\text{Cu}_4(1,3\text{-tpbd})_2(\text{H}_2\text{O})_2(\text{SO}_4)_2](\text{SO}_4)_2$ .<sup>15</sup> Furthermore, substitution of the perchlorate anions in  $[\text{Cu}_2(1,3\text{-tpbd})(\text{H}_2\text{O})_2(\text{ClO}_4)_3](\text{ClO}_4)$  by azide afforded the dicopper(II) complex  $[\text{Cu}_2(1,3\text{-tpbd})(\text{N}_3)_4]$  for which only weak antiferromagnetic coupling was observed ( $J = -2.1 \text{ cm}^{-1}$ ).<sup>16</sup> On the other hand, when oxalate was used as an anion, it caused strong antiferromagnetic coupling between the copper(II) ions ( $J = -366 \text{ cm}^{-1}$ ).<sup>16</sup>

A further study that included copper(II) complexes with the isomeric ligands 1,2-tpbd and 1,4-tpbd, as well as a structurally related ligand capable of forming mononuclear complexes, clearly demonstrated the advantage of the 1,3-tpbd ligand system in mediating ferromagnetic interactions.<sup>17</sup> In spite of the finding that the dicopper(II) complex  $[\text{Cu}_2(1,3\text{-tpbd})\text{Cl}_4]$  did not show ferromagnetic coupling (the magnetic behavior is practically identical to the azide complex  $[\text{Cu}_2(1,3\text{-tpbd})(\text{N}_3)_4]$ ), we observed an intramolecular ferromagnetic interaction in  $[\text{Cu}_2(1,3\text{-tpbd})(\text{H}_2\text{O})_2(\text{S}_2\text{O}_6)]\text{S}_2\text{O}_6$  whose magnitude is very similar to the structurally related complex  $[\text{Cu}_2(1,3\text{-tpbd})(\text{H}_2\text{O})_2(\text{ClO}_4)_3](\text{ClO}_4)$ .<sup>17–19</sup>

Using the same 1,3-tpbd ligand, we thus had achieved magnetic properties ranging from antiferromagnetic to ferromagnetic coupling, which could be tuned by additional coligands. Therefore, we became interested in further developing this system by introducing coligands that would provide larger polynuclear complex units with interesting magnetic properties. Promising candidates as coligands were arsenate and phosphate. Both anions lead to three-dimensional frameworks. Arsenate more recently gained interest in that regard, and different extended structural motifs of iron(III/II) and zinc(II) arsenates have been reported.<sup>20,21</sup>

## RESULTS AND DISCUSSION

**Syntheses.** *N,N,N',N'*-Tetrakis(2-pyridylmethyl)-1,3-benzenediamine (1,3-tpbd) was prepared in good yield according to a literature procedure.<sup>13</sup> The copper(II) complexes were obtained by mixing stoichiometric amounts of the respective copper(II) salts, 1,3-tpbd, and coligands in water/methanol mixtures.

**Molecular Structures of Copper(II) Complexes.**  $[\text{Cu}_4(1,3\text{-tpbd})_2(\text{H}_2\text{O})_4(\text{NO}_3)_4]n(\text{NO}_3)_{4n} \cdot 13n\text{H}_2\text{O}$  (**1**). Previous efforts to obtain single crystals of a nitrate relative of  $[\text{Cu}_2(1,3\text{-tpbd})(\text{H}_2\text{O})_2(\text{ClO}_4)_3]\text{ClO}_4$  were unsuccessful. Whereas the perchlorate anions could be readily substituted, partially or completely, by nitrate ions, the crystal structure obtained could not be refined satisfactorily. Finally, it was recognized that the isolated crystals were quickly deteriorating because of the loss of solvent molecules from the crystal lattice. This problem also caused huge problems in our efforts to obtain a correct elemental

analysis of this or the other complexes described below. This solvent inclusion was observed previously and seems to depend on the anion. Thus it was easily possible to obtain correct data for the elemental analysis for  $[\text{Cu}_2(1,3\text{-tpbd})(\text{H}_2\text{O})_2(\text{ClO}_4)_3]\text{ClO}_4$ , however not for **1** or other related complexes. Keeping the crystals in their mother liquor finally allowed **1** to be structurally characterized. A fragment of the cationic chain of **1** is depicted below in Figure 1. Crystallographic data for **1**, together with

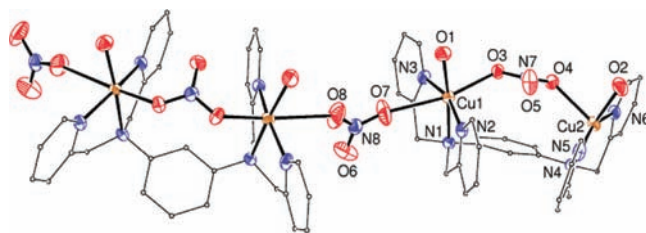


**Figure 1.** Perspective view of a fragment of the copper(II) chain  $[\text{Cu}_4(1,3\text{-tpbd})_2(\text{H}_2\text{O})_4(\text{NO}_3)_4]n^{4n+}$  of **1**. Hydrogen atoms and solvent molecules are omitted for clarity.

those of the remaining structures reported in this work (complexes **2–5**), are listed in Table 1, whereas the main bond lengths and angles of **1–5** are displayed in Table 2.

Complex **1** crystallizes as a copper(II) chain that consists of dinuclear  $[\text{Cu}^{\text{II}}_2(1,3\text{-tpbd})]$  units with intra- and interdimer  $\mu_{1,2}$ -nitrate groups. Each of the copper(II) ions is surrounded by three nitrogen donor atoms, two nitrate ions, and one oxygen atom of a water molecule forming a “4 + 2” distorted octahedral environment quite similar to  $[\text{Cu}_2(1,3\text{-tpbd})(\text{H}_2\text{O})_2(\text{ClO}_4)_3]\text{ClO}_4$ . The distance between the two copper(II) ions in one 1,3-tpbd-containing dicopper(II) unit is 5.798(1) Å, a value which is close to 5.873(1) Å reported earlier for  $[\text{Cu}_2(1,3\text{-tpbd})(\text{H}_2\text{O})_2(\text{ClO}_4)_3]\text{ClO}_4$ .<sup>13</sup> The terminal nitrate ions are weakly coordinated to the copper(II) ions as one terminal nitrate ion has been replaced by a water molecule, an effect which was observed previously for the crystallographically characterized copper(II) acetate complexes with 1,3-tpbd.<sup>15</sup>

Similar polynuclear compounds with copper(II) ions coordinated by nitrogen donors that are intramolecularly linked by nitrate anions were published earlier.<sup>22–24</sup>

$[\text{Cu}_4(1,3\text{-tpbd})_2(\text{AsO}_4)(\text{ClO}_4)_3(\text{H}_2\text{O})](\text{ClO}_4)_2 \cdot 2\text{H}_2\text{O} \cdot 0.5\text{CH}_3\text{OH}$  (**2**). Initially it was attempted to prepare a dinuclear complex by mixing 1,3-tpbd,  $\text{Cu}(\text{ClO}_4)_2 \cdot 6\text{H}_2\text{O}$ , and  $\text{Na}_2\text{HAsO}_4$  in a stoichiometric ratio of 1:2:1. However, given that the tetranuclear copper(II) complex **2** was always isolated as the product, the reaction conditions were modified accordingly. Blue crystals of **2** were analyzed by X-ray diffraction studies, and the tetracopper(II) cationic unit of **2** is shown in Figure 2. Three copper(II) ions Cu(1), Cu(2), and Cu(4) are coordinated by three nitrogen atoms of the 1,3-tpbd ligand, one arsenate oxygen atom, and a perchlorate oxygen atom, whereas for the remaining copper atom Cu(3), the perchlorate anion has been replaced by a water molecule. Each of the four copper(II) ions is “4 + 1” coordinated in a slightly distorted square-pyramidal arrangement. The intramolecular distance between the copper(II) atoms bridged by 1,3-tpbd in **2** [ $\text{Cu}(1) \cdots \text{Cu}(2) = 4.358 \text{ \AA}$ ] is much shorter than in **1**. The separation between the copper(II) atoms (not bridged by 1,3-tpbd) [ $\text{Cu}(1) \cdots \text{Cu}(4) = 6.139 \text{ \AA}$ ] is considerably longer.

The trigonality index parameter  $\tau^{25}$  ranges from 0.08 for Cu(1) to 0.13 for Cu(4) [ $\tau = (\beta - \alpha)/60^\circ$ , with  $\alpha$  and  $\beta$  being the two largest coordination angles around the metal atom;

Table 1. Crystallographic Data of Complexes 1–5

	1	2	3	4	5
empirical formula	C <sub>30</sub> H <sub>45</sub> Cu <sub>2</sub> N <sub>10</sub> O <sub>19.5</sub>	C <sub>60</sub> H <sub>64</sub> AsCl <sub>5</sub> Cu <sub>4</sub> N <sub>12</sub> O <sub>27.5</sub>	C <sub>60.5</sub> H <sub>64</sub> Cl <sub>5</sub> Cu <sub>4</sub> N <sub>12</sub> O <sub>27.5</sub> P	C <sub>108</sub> H <sub>104</sub> Cl <sub>4</sub> Cu <sub>4</sub> N <sub>12</sub> O <sub>32</sub> P <sub>4</sub>	C <sub>177.25</sub> H <sub>166.63</sub> B <sub>4</sub> Cu <sub>4</sub> N <sub>14.63</sub> O <sub>10.38</sub> P
M <sub>r</sub>	984.4	1905.57	1861.62	2601.87	3026.97
temperature [K]	200(2)	200(2)	200(2)	200(2)	200(2)
radiation (λ [Å])	Mo-K <sub>α</sub> 0.71073	Mo-K <sub>α</sub> 0.71073	Mo-K <sub>α</sub> 0.71073	Mo-K <sub>α</sub> 0.71073	Mo-K <sub>α</sub> 0.71073
crystal color and shape	green blocks	blue prisms	blue blocks	turquoise prisms	green rhombuses
crystal size [mm]	0.4 × 0.4 × 0.4	0.3 × 0.2 × 0.045	0.4 × 0.3 × 0.3	0.33 × 0.25 × 0.04	0.24 × 0.18 × 0.08
crystal system	monoclinic	monoclinic	monoclinic	triclinic	monoclinic
space group	C2/c (No. 15)	P2 <sub>1</sub> /c (No. 14)	P2 <sub>1</sub> /c (No. 14)	P $\bar{1}$ (No. 2)	P2 <sub>1</sub> /n (No. 14)
a [Å]	36.691(2)	18.662(2)	18.566(2)	16.312(2)	15.664(2)
b [Å]	8.9054(6)	19.355(2)	19.326(2)	18.040(2)	27.742(3)
c [Å]	24.997(2)	22.504(2)	22.596(2)	22.835(3)	17.767(1)
α [deg]	90.0	90.0	90.0	105.968(2)	90.0
β [deg]	96.667(1)	109.639	109.328(1)	103.670(2)	94.20(1)
γ [deg]	90.0	90.0	90.0	105.645(2)	90.0
V [Å <sup>3</sup> ]	8112.7(9)	7655.9(8)	7650(1)	5080(1)	7700(2)
Z	8	4	4	2	2
ρ <sub>calcd</sub> [g cm <sup>-3</sup> ]	1.613	1.653	1.616	1.474	1.306
μ [mm <sup>-1</sup> ]	1.140	1.787	1.379	0.944	0.632
F(000)	4072	3860	3788	2672	3163
scan range θ [deg]	1.64 to 28.29	1.42 to 28.32	1.42 to 28.32	1.29 to 28.34	3.35 to 25.68
index ranges	−48 ≤ h ≤ 48 −11 ≤ k ≤ 11 −33 ≤ l ≤ 32	−24 ≤ h ≤ 24 −25 ≤ k ≤ 25 −29 ≤ l ≤ 29	−24 ≤ h ≤ 24 −25 ≤ k ≤ 25 −30 ≤ l ≤ 29	−21 ≤ h ≤ 21 −24 ≤ k ≤ 23 −30 ≤ l ≤ 30	−19 ≤ h ≤ 19 −33 ≤ k ≤ 33 −21 ≤ l ≤ 21
reflections collected	46831	92298	90912	59537	69542
unique reflections	9915	18858	18761	27966	14426
R <sub>int</sub>	0.0437	0.1445	0.1039	0.2432	0.1062
data/restraints/parameters	9915/36/572	18858/43/1056	18.761/56/1047	27966/28/1492	14426/1950/1331
goodness-of-fit on F <sup>2</sup>	1.059	1.019	1.018	0.928	1.006
final R indices [I > 2σ(I)]	R1 = 0.0665 wR2 = 0.1927	R1 = 0.0776 wR2 = 0.2133	R1 = 0.0761 wR2 = 0.2150	R1 = 0.1021 wR2 = 0.1957	R1 = 0.0648 wR2 = 0.1225
R indices (all data)	R1 = 0.0924 wR2 = 0.2100	R1 = 0.1967 wR2 = 0.2585	R1 = 0.1667 wR2 = 0.2586	R1 = 0.3480 wR2 = 0.2940	R1 = 0.1495 wR2 = 0.1478
largest diff. peak/hole [e Å <sup>-3</sup> ]	2.087/−0.950	1.496/−1.320	1.556/−2.091	1.639/−0.830	0.653/−0.420

$\tau = 0$  and 1 for ideal square-pyramidal and trigonal-bipyramidal coordination, respectively]. The basal plane of the coordination sphere around each copper(II) ion in **2** is formed by the two pyridyl nitrogen atoms of 1,3-tpbd, which are *trans* to each other, the tertiary amine nitrogen of 1,3-tpbd, and the coordinated arsenate oxygen atom. The apical position is occupied by a perchlorate oxygen atom [Cu(1), Cu(2), and Cu(4)] and the oxygen atom of a coordinated water molecule [Cu(3)].

Only a small number of complexes containing a Cu–O–As moiety have been structurally characterized. For example, Doyle et al. described a copper(II) 2,2'-bipyridine (bipy) complex, in which two copper(II) ions are bridged by two H<sub>2</sub>AsO<sub>4</sub><sup>−</sup> anions.<sup>26</sup> Furthermore, some polyoxometallates are known that contain this binding mode.<sup>27–29</sup> However, to the best of our knowledge **2** represents the first example of a  $\mu_4$ -AsO<sub>4</sub><sup>3−</sup> coordination mode in a copper(II) complex.

[Cu<sub>4</sub>(1,3-tpbd)<sub>2</sub>(PO<sub>4</sub>)(ClO<sub>4</sub>)<sub>3</sub>(H<sub>2</sub>O)](ClO<sub>4</sub>)<sub>2</sub>·2H<sub>2</sub>O·0.5CH<sub>3</sub>OH (**3**). Complex **3** was prepared in an analogous manner to **2**, with Na<sub>2</sub>HAsO<sub>4</sub> being replaced by Na<sub>2</sub>HPO<sub>4</sub>. The blue needles obtained were analyzed by single crystal X-ray diffraction. The molecular structure of the tetracopper(II) cationic unit of **3** (see Figure 3) is isostructural to that of **2**. The separation of the copper(II) ions bridged by 1,3-tpbd [Cu(1)⋯Cu(2) = 4.226 Å] is similar to that found in **2**. However, the separation between

the copper(II) ions not bridged by 1,3-tpbd [Cu(1)⋯Cu(4) = 5.869 Å] is shorter than the distance found in **2**.

Dinuclear copper(II) complexes with bridging phosphate groups are well-known, and they have been used in the past to model the active site of purple acid phosphatases.<sup>30–33</sup> In contrast, the  $\mu_4$ -binding mode is less common and is usually limited to phosphate groups embedded in polyoxometallates<sup>34–37</sup> and sheet-like structures.<sup>38–40</sup> To the best of our knowledge, so far only two other structurally characterized complexes with a discrete  $\mu_4$ -PO<sub>4</sub>–Cu<sub>4</sub> coordination mode (as in **3**) have been reported in the literature.<sup>41,42</sup> Furthermore, it deserves to be noted that Anslyn et al. prepared copper(II) complexes of tripodal ligands, which act as receptors with an extraordinary capacity for binding phosphate and arsenate ions as well as various phosphate esters in neutral aqueous solutions.<sup>43–46</sup>

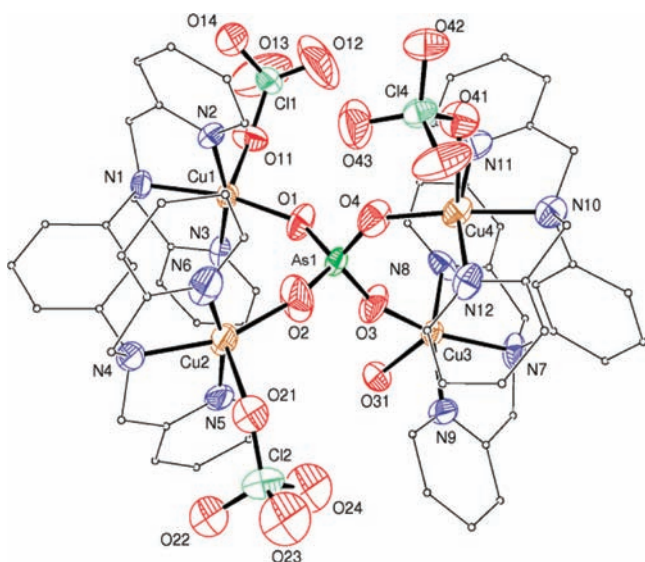
[Cu<sub>2</sub>(1,3-tpbd){(PhO)<sub>2</sub>P(O)<sub>2</sub>}<sub>2n</sub>(ClO<sub>4</sub>)<sub>4n</sub>] (**4**). Introducing sterically demanding organic groups on the phosphate anion should suppress formation of a tetranuclear complex such as **3**. Therefore, diphenylphosphate was chosen as a bridging group. The complex [Cu<sub>2</sub>(1,3-tpbd){(PhO)<sub>2</sub>P(O)<sub>2</sub>}<sub>2n</sub>(ClO<sub>4</sub>)<sub>4n</sub>] (**4**) was obtained by mixing diphenylphosphate, 1,3-tpbd, and Cu(ClO<sub>4</sub>)<sub>2</sub>·6H<sub>2</sub>O in a stoichiometric ratio. The turquoise crystals obtained were analyzed by X-ray diffraction studies and demonstrated that a coordination polymer had formed. A view of the repeating unit including the copper(II) ions connecting the individual units of **4** is shown in Figure 4.

Table 2. Selected Bond Lengths [Å] and Angles of 1–5

atoms	1	atoms	2	3	atoms	4	atoms	5
Cu(1)–O(1)	1.972(3)	Cu(1)–O(1)	1.865(6)	1.874(4)	Cu(1)–O(4)	1.964(7)	Cu(1)–O(11)	1.941(3)
Cu(1)–N(2)	1.972(3)	Cu(1)–N(3)	1.986(7)	1.988(6)	Cu(1)–N(3)	1.970(9)	Cu(1)–N(10)	2.026(3)
Cu(1)–N(3)	1.986(3)	Cu(1)–N(2)	1.990(7)	1.989(5)	Cu(1)–N(2)	1.971(9)	Cu(1)–N(20)	2.002(3)
Cu(1)–N(1)	2.091(3)	Cu(1)–N(1)	2.039(6)	2.061(5)	Cu(1)–N(1)	2.072(9)	Cu(1)–N(1)	2.086(3)
Cu(1)–O(3)	2.313(3)	Cu(1)–O(11)	2.40(2)	2.36(2)	Cu(1)–O(1)	2.168(7)	Cu(1)–O(14 <sup>a</sup> )	2.115(3)
Cu(1)–O(7)	2.729(3)	Cu(2)–O(2)	1.877(6)	1.884(5)	Cu(2)–O(8)	1.958(7)	Cu(2)–O(12)	1.935(3)
Cu(2)–N(5)	1.966(4)	Cu(2)–N(5)	1.978(8)	1.990(8)	Cu(2)–N(6)	1.967(9)	Cu(2)–N(50)	1.991(4)
Cu(2)–N(6)	1.974(4)	Cu(2)–N(6)	2.003(8)	1.988(7)	Cu(2)–N(5)	1.980(9)	Cu(2)–N(40)	1.992(3)
Cu(2)–O(2)	1.979(4)	Cu(2)–N(4)	2.055(7)	2.066(6)	Cu(2)–N(4)	2.057(8)	Cu(2)–N(2)	2.081(3)
Cu(2)–N(4)	2.097(3)	Cu(2)–O(21)	2.383(8)	2.410(8)	Cu(2)–O(5)	2.152(7)	Cu(2)–O(2)	2.221(7)
Cu(2)–O(4)	2.313(3)	Cu(3)–O(3)	1.906(6)	1.885(5)				
Cu(2 <sup>a</sup> )–O(8)	2.792(4)	Cu(3)–N(8)	1.999(7)	1.994(6)				
		Cu(3)–N(9)	2.016(8)	2.011(6)				
		Cu(3)–N(7)	2.050(7)	2.057(5)				
		Cu(3)–O(31)	2.268(6)	2.269(5)				
		Cu(4)–O(4)	1.888(6)	1.871(5)				
		Cu(4)–N(12)	1.994(8)	1.999(6)				
		Cu(4)–N(11)	2.012(8)	2.014(6)				
		Cu(4)–N(10)	2.069(7)	2.051(6)				
		Cu(4)–O(41)	2.369(6)	2.424(5)				
N(2)–Cu(1)–O(1)	94.97(2)	O(1)–Cu(1)–N(3)	94.6(3)	95.7(2)	O(11)–Cu(1)–N(3)	95.4(3)	O(11)–Cu(1)–N(20)	91.0(2)
N(2)–Cu(1)–N(3)	161.13(2)	O(1)–Cu(1)–N(2)	100.7(3)	99.1(2)	O(11)–Cu(1)–N(2)	97.2(3)	O(11)–Cu(1)–N(10)	100.9(2)
O(1)–Cu(1)–N(3)	96.41(2)	N(3)–Cu(1)–N(2)	163.7(3)	164.0(2)	N(20)–Cu(1)–N(2)	165.3(4)	N(20)–Cu(1)–N(10)	161.2(2)
N(2)–Cu(1)–N(1)	83.58(2)	O(1)–Cu(1)–N(1)	168.7(3)	165.7(2)	O(11)–Cu(1)–N(1)	148.2(3)	O(11)–Cu(1)–N(1)	145.6(2)
O(1)–Cu(1)–N(1)	174.09(2)	N(3)–Cu(1)–N(1)	82.0(3)	82.6(2)	N(20)–Cu(1)–N(1)	82.7(4)	N(20)–Cu(1)–N(1)	80.9(2)
N(3)–Cu(1)–N(1)	83.57(2)	N(2)–Cu(1)–N(1)	81.9(3)	81.6(2)	N(10)–Cu(1)–N(1)	82.6(4)	N(10)–Cu(1)–N(1)	81.1(2)
N(2)–Cu(1)–O(3)	106.59(2)	O(1)–Cu(1)–O(11)	96.0(6)	101.4(4)	O(11)–Cu(1)–O(1)	113.8(3)	O(11)–Cu(1)–O(14 <sup>a</sup> )	108.8(2)
O(1)–Cu(1)–O(3)	87.33(2)	N(3)–Cu(1)–O(11)	78.9(6)	78.3(3)	N(20)–Cu(1)–O(1)	91.9(3)	N(20)–Cu(1)–O(14 <sup>a</sup> )	94.6(2)
N(3)–Cu(1)–O(3)	88.95(2)	N(2)–Cu(1)–O(11)	105.1(4)	104.4(4)	N(10)–Cu(1)–O(1)	90.0(3)	N(10)–Cu(1)–O(14 <sup>a</sup> )	95.2(2)
N(1)–Cu(1)–O(3)	98.57(2)	N(1)–Cu(1)–O(11)	94.0(6)	92.2(4)	N(1)–Cu(1)–O(1)	98.0(3)	N(1)–Cu(1)–O(14 <sup>a</sup> )	105.2(2)
N(5)–Cu(2)–N(6)	160.58(2)	O(2)–Cu(2)–N(5)	102.1(3)	99.6(3)	O(8)–Cu(2)–N(6)	99.7(3)	P(1)–O(11)–Cu(1)	150.4(2)
N(5)–Cu(2)–O(2)	94.91(2)	O(2)–Cu(2)–N(6)	92.7(3)	95.5(3)	O(8)–Cu(2)–N(5)	93.6(3)	P(1)–O(14)–Cu(1 <sup>a</sup> )	125.1(2)
N(6)–Cu(2)–O(2)	96.24(2)	N(5)–Cu(2)–N(6)	164.9(3)	164.7(3)	N(6)–Cu(2)–N(5)	165.2(4)	O(12)–Cu(2)–N(50)	93.0(2)
N(5)–Cu(2)–N(4)	83.39(2)	O(2)–Cu(2)–N(4)	159.0(3)	158.6(3)	O(8)–Cu(2)–N(4)	157.8(3)	O(12)–Cu(2)–N(40)	102.3(2)
N(6)–Cu(2)–N(4)	83.94(2)	N(5)–Cu(2)–N(4)	82.8(3)	82.4(3)	N(6)–Cu(2)–N(4)	83.3(4)	N(50)–Cu(2)–N(40)	164.1(2)
O(2)–Cu(2)–N(4)	174.26(2)	N(6)–Cu(2)–N(4)	82.3(3)	82.6(3)	N(5)–Cu(2)–N(4)	82.0(4)	O(12)–Cu(2)–N(2)	162.7(2)
N(5)–Cu(2)–O(4)	106.66(2)	O(2)–Cu(2)–O(21)	102.9(3)	104.9(3)	O(8)–Cu(2)–O(5)	106.6(3)	N(50)–Cu(2)–N(2)	81.6(2)
N(6)–Cu(2)–O(4)	89.46(2)	N(5)–Cu(2)–O(21)	95.8(3)	101.3(3)	N(6)–Cu(2)–O(5)	92.4(3)	N(40)–Cu(2)–N(2)	82.5(2)
O(2)–Cu(2)–O(4)	88.65(2)	N(6)–Cu(2)–O(21)	83.4(3)	77.0(3)	N(5)–Cu(2)–O(5)	89.8(3)	O(12)–Cu(2)–O(2)	105.4(2)
N(4)–Cu(2)–N(4)	97.09(2)	N(4)–Cu(2)–O(21)	96.9(3)	95.5(3)	N(4)–Cu(2)–O(5)	95.2(3)	N(50)–Cu(2)–O(2)	89.0(2)
		O(3)–Cu(3)–N(8)	104.4(3)	101.3(3)			N(40)–Cu(2)–O(2)	91.3(3)
		O(3)–Cu(3)–N(9)	91.8(3)	95.0(2)			N(2)–Cu(2)–O(2)	91.0(2)
		N(8)–Cu(3)–N(9)	163.3(3)	163.2(3)			P(1)–O(12)–Cu(2)	132.9(2)
		O(3)–Cu(3)–N(7)	156.0(3)	154.8(2)				
		N(8)–Cu(3)–N(7)	82.8(3)	82.6(3)				
		N(9)–Cu(3)–N(7)	80.8(3)	80.9(3)				
		O(3)–Cu(3)–O(31)	94.4(3)	97.5(2)				
		N(8)–Cu(3)–O(31)	91.9(3)	91.2(2)				
		N(9)–Cu(3)–O(31)	90.5(3)	90.6(2)				
		N(7)–Cu(3)–O(31)	108.4(3)	107.3(2)				
		O(4)–Cu(4)–N(12)	101.7(3)	100.3(3)				
		O(4)–Cu(4)–N(11)	94.3(3)	96.4(3)				
		N(12)–Cu(4)–N(11)	163.8(3)	163.1(3)				
		O(4)–Cu(4)–N(10)	171.5(3)	171.6(2)				
		N(12)–Cu(4)–N(10)	81.6(3)	81.1(2)				
		N(11)–Cu(4)–N(10)	82.2(3)	82.0(3)				
		O(4)–Cu(4)–O(41)	96.7(2)	101.0(2)				
		N(12)–Cu(4)–O(41)	96.4(3)	96.1(2)				
		N(11)–Cu(4)–O(41)	84.6(2)	82.8(2)				
		N(10)–Cu(4)–O(41)	90.7(2)	87.0(2)				

<sup>a</sup>Denotes a symmetry equivalent atom.





**Figure 2.** Molecular structure of the  $[\text{Cu}_4(1,3\text{-tpbd})_2(\text{AsO}_4)(\text{ClO}_4)_3(\text{H}_2\text{O})]^{2+}$  cation of **2**. Hydrogen atoms and solvent molecules are omitted for clarity.

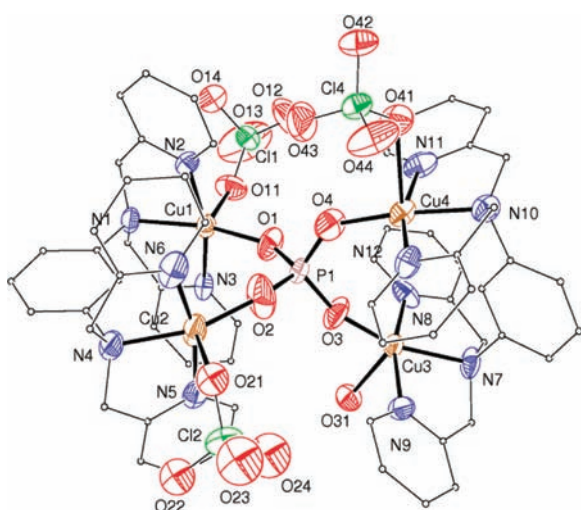


**Figure 3.** Molecular structure of the  $[\text{Cu}_4(1,3\text{-tpbd})_2(\text{PO}_4)(\text{ClO}_4)_3(\text{H}_2\text{O})]^{2+}$  cation of **3**. Hydrogen atoms and solvent molecules are omitted for clarity.

The coordination environment around the crystallographic independent copper(II) ions in **4** is best described as “4 + 1” distorted square-pyramidal with  $\tau$  values<sup>25</sup> of 0.285 at Cu(1) and 0.123 at Cu(2). Interestingly, the diphenylphosphate ligands neither act as bridges between the two adjacent copper(II) ions nor form a tetranuclear unit such as observed in **2** and **3**. Instead, they connect to another dinuclear complex unit, resulting in a chain-like structure, most likely because of the steric crowding of the phenyl groups around the phosphorus atom. An eight-membered ring is formed between the two dinuclear units that is made up by two copper(II) ions, two phosphorus atoms, and four oxygen atoms.

A copper(II) complex forming a similar six-membered ring was published earlier by Chin and co-workers.<sup>47</sup> They studied the phosphate diester cleavage capability of this dicopper(II) complex in a similar fashion to that reported for **6**.<sup>14</sup> The ring formed by two copper-, one phosphorus-, and three oxygen

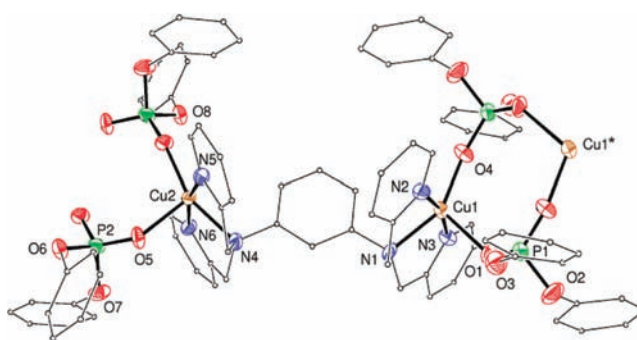


**Figure 4.** Perspective view of a fragment of the  $[\text{Cu}_2(1,3\text{-tpbd})\{(\text{PhO})_2\text{PO}_2\}_2]^{2n+}$  cationic chain of **4**. Hydrogen atoms are omitted for clarity.

atoms plays an important role in the postulated diester cleavage mechanism.<sup>47</sup>

$[\text{Cu}_2(1,3\text{-tpbd})\{(\text{PhO})\text{PO}_3\}_2(\text{H}_2\text{O})_{0.69}(\text{CH}_3\text{CN})_{0.31}]_2(\text{BPh}_4)_4 \cdot \text{Et}_2\text{O} \cdot \text{CH}_3\text{CN}$  (**5**). To relieve some of the steric strain shown in **4**, a monophenylphosphate was used in the synthesis of complex **5**. The molecular structure of the tetracopper(II) cationic part of **5** is shown in Figure 5.

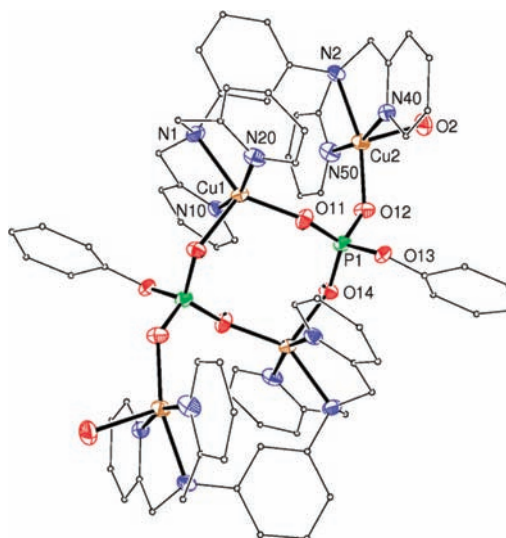


**Figure 5.** Molecular structure of the  $[\text{Cu}_2(1,3\text{-tpbd})\{(\text{PhO})\text{-PO}_3\}_2(\text{H}_2\text{O})_{0.69}(\text{CH}_3\text{CN})_{0.31}]_2^{4+}$  cation of **5**. Hydrogen atoms and solvent molecules are omitted for clarity.

The tetranuclear unit of **5** comprises two 1,3-tpbd molecules, each of them coordinating two copper(II) ions, and two monophenylphosphate anions. As in **4**, an eight-membered ring with two copper(II) ions, two phosphorus atoms, and four oxygen atoms is formed. Moreno et al. and Phuengphai et al. both reported a similar structural motif with the 1,10-phenanthroline ligand (phen) where mono/diphenylphosphate was replaced by dihydrogenphosphate.<sup>48,49</sup> The Cu–O bond lengths reported therein are in good agreement with those of **4** and **5**. Complex **5** crystallizes with an inversion center located in the middle of the Cu–P–O eight-membered ring. The four copper(II) ions are connected via the monophenylphosphate groups resulting in a tetranuclear complex, which is built up of two dinuclear symmetry-related units.

The coordination environment around the copper(II) ions in one of the two units in **5** is again “4 + 1” distorted square-pyramidal.

The distortion differs remarkably for Cu(1) and Cu(2). The trigonality index parameter  $\tau^{25}$  has values of 0.263 [at Cu(1)] and 0.023 [at Cu(2)].

$[\text{Cu}_2(2,6\text{-tpcd})(\text{H}_2\text{O})\text{Cl}](\text{ClO}_4)_2 \cdot 2\text{H}_2\text{O}$  (**6**). The crystal structure of the dinuclear complex **6** was previously reported.<sup>14</sup> Its structure is reproduced in Figure 6, the pertinent feature being

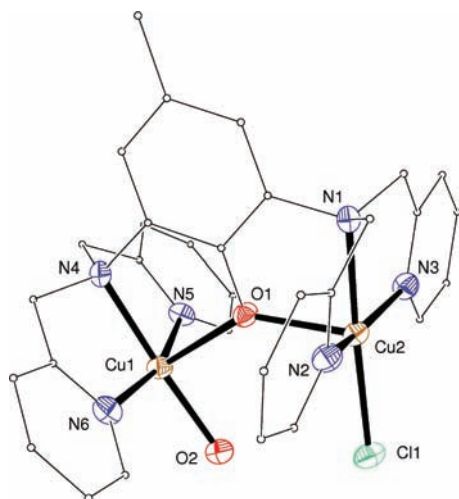


**Figure 6.** Molecular structure of  $[\text{Cu}_2(2,6\text{-tpcd})(\text{H}_2\text{O})\text{Cl}]^{2+}$  cation of **6**. Hydrogen atoms, solvent molecules, and uncoordinated anions are omitted for clarity.

that the phenolate oxygen atom occupies the apical position at each copper(II) ion. The magnetic properties of this compound are reported here as a model compound in the interpretation of the magnetic properties of **2–4**.

**Magnetic Properties of 2, 3, 4, and 6.** The ferromagnetic coupling observed in  $[\text{Cu}_2(1,3\text{-tpbd})(\text{H}_2\text{O})_2(\text{ClO}_4)_3]\text{ClO}_4$ , following the spin polarization mechanism, was successfully interpreted using density functional theory (DFT) calculations.<sup>15</sup> This finding is in good agreement with a related benzenediamine-based dinuclear complex that also showed ferromagnetic coupling ( $J = +16.8 \text{ cm}^{-1}$ ) between two copper(II) ions over a large distance.<sup>50</sup> More recently, ferromagnetic coupling has been observed in *m*-phenylenediamine-bridged tris(2-aminoethyl)-amine copper(II) complex units<sup>51</sup> and oligo-*m*-phenylene-oxalamide copper(II) mesocates.<sup>52</sup> These last examples can be viewed as electro-switchable ferromagnetic metal organic wires. For the nitrate complex **1**, the fast deterioration that it undergoes because of the loss of solvent precludes its magnetic study. However, a structural comparison between **1** and  $[\text{Cu}_2(1,3\text{-tpbd})(\text{H}_2\text{O})_2(\text{ClO}_4)_3]\text{ClO}_4$  suggests that most likely a ferromagnetic coupling would occur between the copper(II) ions through the 1,3-tpbd bridging ligand. Here the loss of solvent molecules in the copper(II) complex can cause subtle structural changes, which prevent detailed magnetic analysis, a situation experienced previously for the acetate system.<sup>15</sup> Therefore, magnetic measurements were only performed on **2, 3, 4, and 6**.

The magnetic properties of complex **6** (Figure 6) under the form of the  $\chi_M T$  versus  $T$  plot [ $\chi_M$  is the magnetic susceptibility per two copper(II) ions] are shown in Figure 7. At room temperature,  $\chi_M T$  is equal to  $0.80 \text{ cm}^3 \text{ mol}^{-1} \text{ K}$ , a value which is as expected for two magnetically isolated spin doublets ( $\chi_M T = 0.75 \text{ cm}^3 \text{ mol}^{-1} \text{ K}$  with  $g = 2.0$ ). A Curie law behavior is observed upon cooling until about 30 K.  $\chi_M T$  decreases sharply in the low temperature domain and a value of  $0.55 \text{ cm}^3 \text{ mol}^{-1} \text{ K}$  at

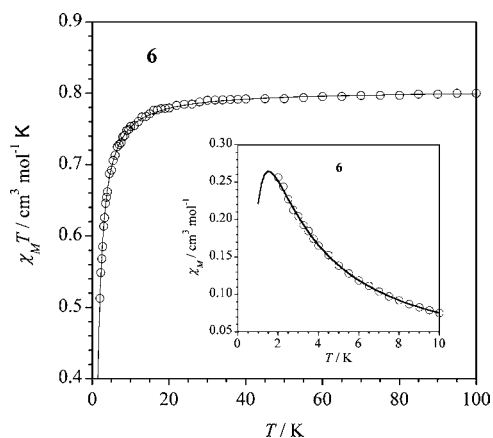


**Figure 7.** Temperature dependence of the  $\chi_M T$  product for **6**: (○) experimental data; (black lines) best-fit curves through eq (1) (see text). The inset shows the  $\chi_M$  versus  $T$  plot for  $T < 10 \text{ K}$ .

1.9 K is attained. A maximum of the magnetic susceptibility is quasi reached, the temperature of such a maximum being slightly below 1.9 K (see the inset of Figure 7). These features are consistent with the occurrence of a weak intramolecular antiferromagnetic interaction between two local spin doublets leading to a singlet ground spin state.

In light of the discrete dinuclear structure of compound **6**,<sup>14</sup> its magnetic data were analyzed through a simple Bleaney–Bowers expression (eq 1), which was derived through the isotropic Hamiltonian  $\mathbf{H} = -J\mathbf{S}_1 \cdot \mathbf{S}_2$

$$\chi_M = (2N\beta^2 g^2 / kT) [3 + \exp(-J/kT)]^{-1} \quad (1)$$

where  $J$  and  $g$  are the singlet–triplet energy gap and the average  $g$  factor for the dicopper(II) unit, and  $N$ ,  $\beta$ , and  $k$  have their usual meanings. Least-squares fitting leads to the following parameters:  $J = -1.70(1) \text{ cm}^{-1}$ ,  $g = 2.07(1)$ , and  $R = 1.2 \times 10^{-5}$  ( $R$  is the agreement factor defined as  $\sum[(\chi_M)_{\text{obs}} - (\chi_M)_{\text{calc}}]^2 / \sum[(\chi_M)_{\text{obs}}]^2$ ). The computed curve matches well the experimental one in the temperature range investigated. The small value of the weak intramolecular magnetic interaction in **6** can be understood by looking at the respective orientation of the magnetic orbitals involved. In fact, each copper(II) ion of this compound is found in a square-pyramidal environment, the basal plane being defined by the N(4), N(5), N(6), and O(2) [at Cu(1)] and N(1), N(2), N(3), and Cl(1) [at Cu(2)] set of atoms (see Figure 6). A phenolate oxygen atom [O(1)] fills the apical position, the copper to O(1) bond distances being longer than 2.1 Å. In such a case, the unpaired electron at each copper(II) ion is located in the equatorial plane (the magnetic orbital) and a weak overlap is predicted between the two magnetic orbitals through the phenolate oxygen atom because of the small spin density at the apical position. Also the magnetic coupling through the long  $\sigma$  in-plane Cu(1)–N(4)–C(17)–C(18)–C(13)–N(3)–Cu(2) pathway [*syn-syn* conformation according to the relative orientation of the Cu(1)–N(4) and Cu(2)–N(1) bonds] is expected to be very weak.<sup>15</sup> The low efficiency of both exchange pathways in **6** accounts for the weak magnetic coupling observed.

The magnetic properties of complex **4** under the form of the  $\chi_M T$  versus  $T$  plot [ $\chi_M$  is the magnetic susceptibility per two copper(II) ions] are shown in Figure 8. At room temperature,  $\chi_M T$  is equal to  $0.80 \text{ cm}^3 \text{ mol}^{-1} \text{ K}$ , a value which is as expected for two magnetically noninteracting spin doublets. A Curie law behavior is observed upon cooling until about 70 K and

afterwards  $\chi_M T$  decreases sharply at lower temperatures to attain a value of  $0.17 \text{ cm}^3 \text{ mol}^{-1} \text{ K}$  at 1.9 K. A maximum of the magnetic susceptibility occurs at 3.5 K (see the inset of Figure 8).

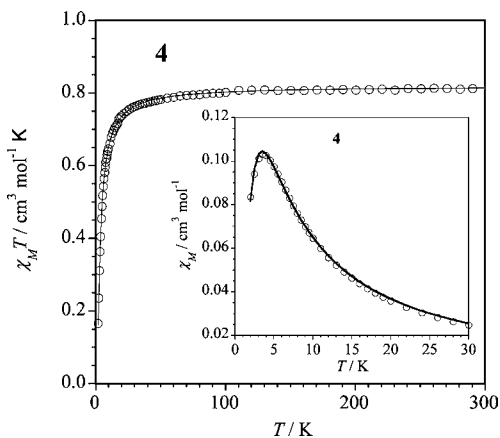


**Figure 8.** Temperature dependence of the  $\chi_M T$  product for **4**: (O) experimental data; (black lines) best-fit curves through eq. (2) (see text). The inset shows the  $\chi_M$  versus  $T$  in the vicinity of the maximum.

These features are characteristic of an overall weak antiferromagnetic behavior.

In agreement with the chain structure of **4** where the regular alternating bis-terdentate 1,3-tpbd and doubly bis-monodenate  $(\text{PhO})_2\text{P}(\text{O})_2$  bridges occurs, its magnetic data were analyzed through the alternating chain spin exchange model (eq 2) and the development of Hatfield et al.<sup>53</sup>

$$\mathbf{H} = -J \sum (\mathbf{S}_{2i} \cdot \mathbf{S}_{2i-1} + \alpha \mathbf{S}_{2i} \cdot \mathbf{S}_{2i+1}) \quad (2)$$

where  $J$  and  $\alpha$  are the exchange coupling and alternation parameter, respectively. Least-squares fit minimizing  $R = \sum [(\chi_M)_{\text{obs}} - (\chi_M)_{\text{calc}}]^2 / \sum [(\chi_M)_{\text{obs}}]^2$  led to the following set of values:  $J = -3.90(1) \text{ cm}^{-1}$ ,  $\alpha J = -1.79(2) \text{ cm}^{-1}$ ,  $g = 2.09(1)$ , and  $R = 2.3 \times 10^{-5}$ . The calculated curve reproduces the magnetic data very well in the whole temperature range investigated. The two intrachain magnetic couplings in **4** are weak and antiferromagnetic, and their assignment to the two exchange pathways involved is not evident at first sight. Their weakness is not surprising bearing in mind the two exchange pathways involved: the extended bis-terdentate 1,3-tpbd molecule, which links equatorial positions at the Cu(1) and Cu(2) [ $\text{Cu}(1) \cdots \text{Cu}(2) = 8.12 \text{ \AA}$ ] and the pair of bis-monodenate  $(\text{PhO})_2\text{P}(\text{O})_2$  bridges connecting an equatorial position of a copper atom with the apical one of the adjacent copper [ $\text{Cu}(1) \cdots \text{Cu}(1A) = 4.59 \text{ \AA}$  and  $\text{Cu}(2) \cdots \text{Cu}(2A) = 4.67 \text{ \AA}$ ].

The former one is a  $\sigma$  in-plane exchange pathway as in **6**, the  $\text{Cu}(1)-\text{N}(1)-\text{C}(13)-\text{C}(18)-\text{C}(17)-\text{N}(4)-\text{Cu}(2)$  fragment exhibiting the *anti-anti* conformation instead of the *syn-syn* occurring for such a fragment in **6**. Most likely, the weaker antiferromagnetic interaction [ $\alpha J = -1.79(2) \text{ cm}^{-1}$ ] is mediated by this bridging pathway, whereas the somewhat larger antiferromagnetic coupling [ $J = -3.90(1) \text{ cm}^{-1}$ ] would involve the double equatorial-apical  $\mu_{1,2}-\text{O}-\text{P}-\text{O}$  skeleton involving a much shorter copper–copper separation.

The magnetic properties of the complexes **2** and **3** under the form of  $\chi_M T$  versus  $T$  plots [ $\chi_M$  is the magnetic susceptibility per four copper(II) ions] are shown in Figure 9. At room temperature,  $\chi_M T$  for **2** and **3** is about  $1.60 \text{ cm}^3 \text{ mol}^{-1} \text{ K}$ , a value which is as expected for four magnetically isolated spin

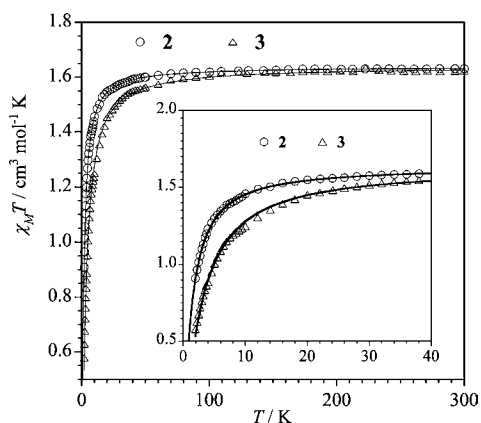


**Figure 9.** Temperature dependence of the  $\chi_M T$  product for **2** and **3**: (O,  $\Delta$ ) experimental data; (black lines) best-fit curves through eq. (3) (see text). The inset shows a detail of the low temperature region.

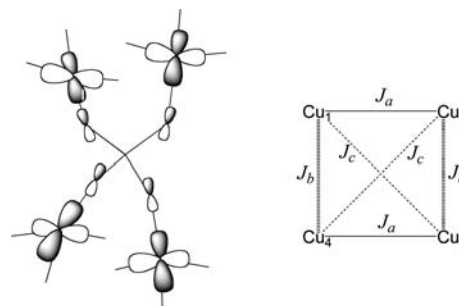
doublets [ $\chi_M T = \text{cm}^3 \text{ mol}^{-1} \text{ K}$  with  $g = 2.0$ ]. Upon cooling, a Curie law behavior is observed until about 100 K, which is followed by an abrupt decrease of  $\chi_M T$  to reach values of  $0.9$  (**2**) and  $0.55 \text{ cm}^3 \text{ mol}^{-1} \text{ K}$  (**3**) at 1.9 K. No maximum in the magnetic susceptibility is observed for **2** and **3** in the temperature range explored. This decrease of  $\chi_M T$  in the low temperature domain is due to relatively weak intramolecular antiferromagnetic interactions.

In agreement with the tetrahedral arrangement of the four copper(II) ions in **2** and **3**, their magnetic data were analyzed through the isotropic spin Hamiltonian of eq. (3).

$$\begin{aligned} \mathbf{H} = & -J_a(\mathbf{S}_1 \cdot \mathbf{S}_2 + \mathbf{S}_3 \cdot \mathbf{S}_4) - J_b(\mathbf{S}_1 \cdot \mathbf{S}_4 + \mathbf{S}_2 \cdot \mathbf{S}_3) \\ & - J_c(\mathbf{S}_1 \cdot \mathbf{S}_3 + \mathbf{S}_2 \cdot \mathbf{S}_4) - g\beta H(\mathbf{S}_1 + \mathbf{S}_2 + \mathbf{S}_3 + \mathbf{S}_4) \quad (3) \end{aligned}$$

where  $J_a$ ,  $J_b$ , and  $J_c$  are the magnetic coupling parameters (see Scheme 2, right) and  $g$  is the average Landé factor which is

**Scheme 2.** (Left) Orbital Picture Illustrating the Exchange Pathways through the  $\mu_4-\text{XO}_4$  with  $\text{X} = \text{As}$  (**2**) and  $\text{P}$  (**3**); (Right) Intramolecular Spin Coupling Pattern in **2** and **3**



assumed to be identical for the four copper(II) ions. Numerical matrix diagonalization techniques using a Fortran program<sup>54</sup> (conducting extensive mappings with the aim of locating the global minimum of each system among a large number of local minima) led to the following set of parameters through least-squares fitting of the data:  $J_a = J_b = J_c = -1.11(1) \text{ cm}^{-1}$ ,  $g = 2.09(1)$ , and  $R = 1.6 \times 10^{-6}$  (**2**),  $J_a = J_b = J_c = -2.27(1) \text{ cm}^{-1}$ ,  $g = 2.09(1)$  and  $R = 1.5 \times 10^{-6}$  (**3**) ( $R$  is the agreement factor defined as  $R = \sum [(\chi_M T)_{\text{obs}} - (\chi_M T)_{\text{calc}}]^2 / \sum [(\chi_M T)_{\text{obs}}]^2$ ). An excellent agreement between the experimental data and the calculated curves is obtained in the two cases.



It deserves to be noted that although we tried different sets of starting values for the  $J_i$  parameters (even of different nature), the best fit is always achieved with the same value for the three magnetic couplings in each complex. This means that the magnetic coupling through the  $\mu_4$ -XO<sub>4</sub> motif is dominant and then, the interaction through the extended 1,3-tpbd involving the pairs Cu(1)/Cu(2) and Cu(3)/Cu(4) pairs would be negligible. Looking at the structure of **2** and **3**, this can be easily understood because of the common Cu–O–X–O–Cu' [X = As (**2**) and P (**3**)] five-atoms-set involved in the intramolecular exchange pathways connecting equatorial positions (see the orbital picture in Scheme 2). The somewhat shorter values of the intramolecular Cu...Cu' separation for **3** with respect to those in **2** (dictated by the shorter P–O bond lengths compared to the As–O ones) would account for the slightly larger antiferromagnetic coupling in **3**.

Finally, a brief comment concerning the weak magnetic interactions in these two complexes is warranted. To the best of our knowledge, the case of **2** is the first magneto-structurally characterized example of a  $\mu_4$ -AsO<sub>4</sub>-bridged copper(II) complex, and this precludes any comparison. A similarly related complex is the copper(II) complex  $\{[\text{Cu}(\text{bipy})(\text{H}_2\text{AsO}_4)](\mu_{1,2}\text{-H}_2\text{AsO}_4)\}$  where a very weak antiferromagnetic coupling between the copper(II) ions ( $J = -0.58 \text{ cm}^{-1}$ ) is mediated by a pair of bis-monodentate dihydrogenarsenate bridges, the copper–copper separation being 5.287 Å.<sup>26</sup> The case of complex **3** is also a special one because no correlation between the structural parameters and the magnetic coupling exists and the magnetic coupling through the Cu–O–P–O–Cu pathway covers a wide range of significant values either negative or positive.<sup>55</sup> In fact, only two other structurally characterized complexes with a tetrakis-monodentate-coordination mode of the phosphate group are known but their magnetic properties were not investigated.<sup>41,42</sup>

## CONCLUSIONS

The copper(II) 1,3-tpbd complexes **1–5** exhibit interesting structural properties. Two of them (**2** and **3**) show rare or even unique coordination modes of copper(II) ions with the arsenate (**2**) or phosphate (**3**) coligands. Furthermore, an eight-membered ring between two copper(II) ions and two phosphate molecules occurs in complexes **4** and **5**. The study of the magnetic behavior of **2**, **3**, **4**, and the related compound  $[\text{Cu}_2(2,6\text{-tpcd})(\text{H}_2\text{O})\text{Cl}(\text{ClO}_4)_2]$  (**6**) shows that the bis-terdentate 1,3-tpbd, 2,6-tpcd, bis-monodentate O–P–O, and tetrakis-monodentate-XO<sub>4</sub><sup>3-</sup> (X = P and As) bridges appear as poor mediators of magnetic interactions between the copper(II) atoms in these species. Simple magnetic orbital considerations, which are based on the structural knowledge and previous theoretical calculations, account for the weak magnetic interactions. Larger polynuclear copper(II) 1,3-tpbd complexes containing anionic coligands were prepared, although the magnetic interactions in these new compounds turned out to be weak and antiferromagnetic. Finally, this work demonstrates methods to increase the nuclearity and/or dimensionality of the 1,3-tpbd-containing copper(II) complexes, the achievement of stronger magnetic couplings being the goal to be achieved by varying the nature of the coligand.

## EXPERIMENTAL SECTION

**Materials.** All chemicals were obtained from commercial sources and used without further purification. The 1,3-tpbd ligand was prepared according to a literature procedure.<sup>13</sup>

**Caution!** The syntheses and procedures described below involve compounds that contain perchlorate ions, which can detonate explosively

and without warning. Although we have not encountered any problems with the compounds used in this study, they should be handled with extreme caution.

**Syntheses of Copper Complexes 1–5.**  $[\text{Cu}_4(1,3\text{-tpbd})_2(\text{H}_2\text{O})_4(\text{NO}_3)_4]_n(\text{NO}_3)_{4n} \cdot 13n\text{H}_2\text{O}$  (**1**). 1,3-tpbd (328.8 mg, 0.680 mmol) dissolved in methanol (15 mL) was added to an aqueous solution (10 mL) of  $\text{Cu}(\text{NO}_3)_2 \cdot 3\text{H}_2\text{O}$  (328.4 mg; 1.360 mmol). The reaction mixture was stirred for 5 min during which time the solution turned to a dark green color. Single crystals of **1** were obtained after two days. UV/vis (MeOH)  $\lambda_{\text{max}} = 383 \text{ nm}$  ( $\epsilon = 2800 \text{ M}^{-1} \text{ cm}^{-1}$ ), 684 nm ( $\epsilon = 600 \text{ M}^{-1} \text{ cm}^{-1}$ ).

$[\text{Cu}_4(1,3\text{-tpbd})_2(\text{AsO}_4)(\text{ClO}_4)_3(\text{H}_2\text{O})](\text{ClO}_4)_2 \cdot 2\text{H}_2\text{O} \cdot 0.5\text{CH}_3\text{OH}$  (**2**) /  $[\text{Cu}_4(1,3\text{-tpbd})_2(\text{PO}_4)(\text{ClO}_4)_3(\text{H}_2\text{O})](\text{ClO}_4)_2 \cdot 2\text{H}_2\text{O} \cdot 0.5\text{CH}_3\text{OH}$  (**3**) /  $[\text{Cu}_2(1,3\text{-tpbd})_2(\text{PhO})_2(\text{PO}_4)_2]_n(\text{ClO}_4)_{4n}$  (**4**). 1,3-tpbd (100.0 mg, 0.21 mmol) dissolved in methanol (15 mL) was added to aqueous solutions (5 mL) of  $\text{Cu}(\text{ClO}_4)_2 \cdot 6\text{H}_2\text{O}$  (155 mg, 0.42 mmol) and  $\text{Na}_2\text{HAsO}_4$  (65.5 mg, 0.21 mmol) for **2**,  $\text{Cu}(\text{ClO}_4)_2 \cdot 6\text{H}_2\text{O}$  (155.0 mg, 0.42 mmol) and  $\text{Na}_2\text{HPO}_4$  (56.3 mg, 0.21 mmol) for **3**, and  $\text{Cu}(\text{ClO}_4)_2 \cdot 6\text{H}_2\text{O}$  (155.0 mg, 0.42 mmol) and diphenylphosphate (52.5 mg; 0.21 mmol) for **4**. The green reaction solutions were each stirred for 5 min. Crystals suitable for X-ray diffraction were formed after two days. Intense blue crystals of **2** (UV/vis (MeOH)  $\lambda_{\text{max}} = 380 \text{ nm}$  (shoulder,  $\epsilon = 900 \text{ M}^{-1} \text{ cm}^{-1}$ ), 713 nm ( $\epsilon = 500 \text{ M}^{-1} \text{ cm}^{-1}$ )) and of **3** (UV/vis (MeOH)  $\lambda_{\text{max}} = 706 \text{ nm}$  ( $\epsilon = 600 \text{ M}^{-1} \text{ cm}^{-1}$ )), and light blue crystals of **4** (UV/vis (MeCN)  $\lambda_{\text{max}} = 308 \text{ nm}$  (shoulder,  $\epsilon = 4100 \text{ M}^{-1} \text{ cm}^{-1}$ ), 379 nm ( $\epsilon = 1500 \text{ M}^{-1} \text{ cm}^{-1}$ ), 734 nm ( $\epsilon = 500 \text{ M}^{-1} \text{ cm}^{-1}$ )).

$[\text{Cu}_2(1,3\text{-tpbd})_2(\text{PhO})\text{PO}_3(\text{H}_2\text{O})_{0.69}(\text{CH}_3\text{CN})_{0.31}]_2(\text{BPh}_4)_4 \cdot \text{Et}_2\text{O} \cdot \text{CH}_3\text{CN}$  (**5**). Aqueous solutions (5 mL) of  $\text{Cu}(\text{ClO}_4)_2 \cdot 6\text{H}_2\text{O}$  (78.4 mg, 0.210 mmol) and the sodium salt of phenylphosphate (27.0 mg, 0.105 mmol) were added to a mixture of 1,3-tpbd (50.0 mg, 0.105 mmol) and  $\text{NaBPh}_4$  dissolved in methanol. The turquoise precipitate was filtered and dissolved in  $\text{CH}_3\text{CN}$ . Crystals suitable for X-ray diffraction analyses were obtained by slow diffusion of diethyl ether into the solution. (UV/vis (MeCN)  $\lambda_{\text{max}} = 380 \text{ nm}$  ( $\epsilon = 1700 \text{ M}^{-1} \text{ cm}^{-1}$ ), 701 nm ( $\epsilon = 500 \text{ M}^{-1} \text{ cm}^{-1}$ )).

**Magnetic Measurements.** Variable-temperature (1.9–300 K) magnetic susceptibility measurements on polycrystalline samples of **2**, **3**, **4**, and **6** were collected with a SQUID susceptometer under applied dc magnetic fields of 1 T ( $T \geq 100 \text{ K}$ ) and 500 G ( $T < 100 \text{ K}$ ). Corrections of the diamagnetism for the constituent atoms of **2**, **3**, **4**, and **6** were done by means of the Pascal's constants.<sup>56</sup> Corrections for the sample holder as well as for the temperature-independent paramagnetism [ $60 \times 10^{-6} \text{ cm}^3 \text{ mol}^{-1} \text{ K}$  per copper(II) ion] were also applied.

**X-ray Crystallographic Studies.** Intensity data of **1–4** were collected with a Siemens SMART CCD 1000 diffractometer by the  $\omega$ -scan technique collecting a full sphere of data with irradiation times of 10 to 20 s per frame and  $\Delta\omega$  ranges between  $0.3^\circ$  and  $0.45^\circ$ . The collected reflections were corrected for absorption, Lorentz, and polarization effects.<sup>57</sup> All structures were solved by direct methods and refined by least-squares techniques using the SHELX-97 program package.<sup>58</sup> The hydrogen atoms were positioned geometrically, and all non-hydrogen atoms, if not mentioned otherwise, were refined anisotropically. Further data collection parameters are summarized in Table 1.

Intensity data of **5** were collected with a Bruker-Nonius Kappa CCD diffractometer. Absorption effects were corrected by semi-empirical methods based on equivalent reflections.<sup>57</sup> The structure was solved by direct methods; full-matrix least-squares refinement was carried out on  $F^2$  using SHELXTL NT 6.12.<sup>57</sup> All non-hydrogen atoms were refined anisotropically. The high residual electron density in **5** is due to the high amount of solvent molecules and the poor quality of the crystals. Hydrogen atoms were geometrically positioned, their isotropic displacement parameters were tied to those of their corresponding carrier atoms by a factor of 1.2 or 1.5. Both of the  $\text{BPh}_4^-$  anions show disordered phenyl groups. SIMU and SAME restraints were applied in the refinement of these anions. The coligand at Cu(2) is disordered. The sixth coordination site is either occupied by an aqua ligand [O(2), 69(2)%] for which no hydrogen atoms have been included in the structural model or by an acetonitrile molecule [N(S20)–C(S22), 31(2)%]. A disordered  $\text{Et}_2\text{O}$  molecule [O(S00)–C(S04)] is partially present when the aqua ligand is coordinated to



Cu(2). SIMU, SADI, SAME, and ISOR restraints were applied in the treatment of this disordered part of the structure.

CCDC nos. 661254 (1), 661255(2), 661256(3), 661257(4), and 658344 (5) contain the supplementary crystallographic data for this paper. These data can be obtained free of charge at [www.ccdc.cam.ac.uk/conts/retrieving.html](http://www.ccdc.cam.ac.uk/conts/retrieving.html) [or from the Cambridge Crystallographic Data Centre, 12, Union Road, Cambridge CB2 1EZ, U.K.; Fax: (internat.) +44-1223-336-033; E-mail: [deposit@ccdc.cam.ac.uk](mailto:deposit@ccdc.cam.ac.uk)].

## AUTHOR INFORMATION

### Corresponding Author

\*E-mail: [Miguel.Julve@uv.es](mailto:Miguel.Julve@uv.es) (M.J.); [Siegfried.Schindler@chemie.uni-giessen.de](mailto:Siegfried.Schindler@chemie.uni-giessen.de) (S.S.)

### Present Address

<sup>†</sup>European Commission Joint Research Centre, Institute for Transuranium Elements, Hermann-von-Helmholtz-Platz 1, 76344 Eggenstein-Leopoldshafen, Germany

## ACKNOWLEDGMENTS

This work was supported by the Ministerio Español de Ciencia e Innovación through projects CTQ2010-15364 and Molecular Nanoscience (Consolider Ingenio CSD-2007-00010).

## REFERENCES

- (1) Verdaguer, M.; Linert, W. *Molecular Magnets: Recent Highlights*, 1st ed.; Springer: Wien, Austria, 2003; p 220.
- (2) Kahn, O. *Molecular Magnetism*; Wiley VCH: Weinheim, Germany, 1993.
- (3) Willet, R. D.; Gatteschi, D.; Kahn, O. *Magneto-Structural Correlations in Exchange Systems*; Reidel: Dordrecht, The Netherlands, 1985.
- (4) Ruiz, E.; Alemany, P.; Alvarez, S.; Cano, J. *J. Am. Chem. Soc.* **1997**, *119*, 1297–1303.
- (5) Ruiz, E.; Alemany, P.; Alvarez, S.; Cano, J. *Inorg. Chem.* **1997**, *36*, 3683–3688.
- (6) Ruiz, E.; Cano, J.; Alvarez, S.; Alemany, P. *J. Am. Chem. Soc.* **1998**, *120*, 11122–11129.
- (7) Cano, J.; Alemany, P.; Alvarez, S.; Verdaguer, M.; Ruiz, E. *Chem.—Eur. J.* **1998**, *4*, 476–484.
- (8) Cano, J.; Ruiz, E.; Alemany, P.; Lloret, F.; Alvarez, S. *J. Chem. Soc., Dalton Trans.* **1999**, 1669–1676.
- (9) Rodríguez-Forteza, A.; Alemany, P.; Alvarez, S.; Ruiz, E. *Chem.—Eur. J.* **2001**, *7*, 627–637.
- (10) Ruiz, E.; Rodríguez-Forteza, A.; Alvarez, S.; Verdaguer, M. *Chem.—Eur. J.* **2005**, *11*, 2135–2144.
- (11) Venegas-Yazigi, D.; Aravena, D.; Spodine, E.; Ruiz, E.; Alvarez, S. *Coord. Chem. Rev.* **2010**, *254*, 2086–2095.
- (12) Cañadillas-Delgado, L.; Fabelo, O.; Pasán, J.; Delgado, F. S.; Lloret, F.; Julve, M.; Ruiz-Peréz, C. *Dalton Trans.* **2010**, *39*, 7286–7293.
- (13) Schindler, S.; Szalda, D. J.; Creutz, C. *Inorg. Chem.* **1992**, *31*, 2255–2264.
- (14) Foxon, S.; Xu, J.-Y.; Turba, S.; Leibold, M.; Hampel, F.; Heinemann, F. W.; Walter, O.; Würtele, C.; Holthausen, M.; Schindler, S. *Eur. J. Inorg. Chem.* **2007**, 429–443.
- (15) Foxon, S. P.; Torres, G. R.; Walter, O.; Pedersen, J. Z.; Toftlund, H.; Hüber, M.; Falk, K.; Haase, W.; Cano, J.; Lloret, F.; Julve, M.; Schindler, S. *Eur. J. Inorg. Chem.* **2004**, 335–343.
- (16) Foxon, S. P.; Walter, O.; Koch, R.; Rupp, H.; Müller, P.; Schindler, S. *Eur. J. Inorg. Chem.* **2004**, 344–348.
- (17) Turba, S.; Walter, O.; Schindler, S.; Nielsen, L. P.; Hazell, A.; J. McKenzie, C.; Lloret, F.; Cano, J.; Julve, M. *Inorg. Chem.* **2008**, *47*, 9612–9623.
- (18) Li, D.; Tian, J.; Kou, Y.; Huang, F.; Chen, G.; Gu, W.; Liu, X.; Liao, D.; Cheng, P.; Yan, S. *Dalton Trans.* **2009**, 3574–3583.
- (19) Li, D.-D.; Huang, F.-P.; Chen, G.-J.; Gao, C.-Y.; Tian, J.-L.; Gu, W.; Liu, X.; Yan, S.-P. *J. Inorg. Biochem.* **2010**, *104*, 431–441.
- (20) Chakrabarti, S.; Natarajan, S. *Angew. Chem., Int. Ed.* **2002**, *41*, 1224–1226.
- (21) Rao, V. K.; Chakrabarti, S.; Natarajan, S. *Inorg. Chem.* **2007**, *46*, 10781–10790.
- (22) de Hoog, P.; Gamez, P.; Lüken, M.; Roubeau, O.; Krebs, B.; Reedijk, J. *Inorg. Chim. Acta* **2004**, *357*, 213–218.
- (23) Gómez-Saiz, P.; García-Tojal, J.; Díez-Gómez, V.; Gil-García, R.; Pizarro, J. L.; Arriortua, M. I.; Rojo, T. *Inorg. Chem. Commun.* **2005**, *8*, 259–262.
- (24) Grove, H.; Sletten, J.; Julve, M.; Lloret, F.; Cano, J. *J. Chem. Soc., Dalton Trans.* **2001**, 259–265.
- (25) Addison, A. W.; Rao, T. N.; Reedijk, J.; van Rijn, J.; Verschoor, G. C. *J. Chem. Soc., Dalton Trans.* **1984**, 1349–1356.
- (26) Doyle, R. P.; Kruger, P. E.; Julve, M.; Lloret, F.; Nieuwenhuyzen, M. *CrystEngComm* **2002**, *4*, 13–16.
- (27) Hou, Y.; Wang, S.; Shen, E.; Xiao, D.; Wang, E.; Li, Y.; Xu, L.; Hu, C. *J. Mol. Struct.* **2004**, *689*, 81–88.
- (28) Li, Y.; De, G.; Yuan, M.; Wang, E.; Huang, R.; Hu, C.; Hu, N.; Jia, H. *Dalton Trans.* **2003**, 331–334.
- (29) Soumahoro, T.; Burkholder, E.; Ouellette, W.; Zubieta, J. *Inorg. Chim. Acta* **2005**, *358*, 606–616.
- (30) Krebs, B.; Schepers, K.; Bremer, B.; Henkel, G.; Althaus, E.; Mueller-Warmuth, W.; Griesar, K.; Haase, W. *Inorg. Chem.* **1994**, *33*, 1907–1914.
- (31) Lim, J.-S.; Aquino, M. A. S.; Sykes, A. G. *Inorg. Chem.* **1996**, *35*, 614–618.
- (32) True, A. E.; Scarrow, R. C.; Randall, C. R.; Holz, R. C.; Que, L. *J. Am. Chem. Soc.* **1993**, *115*, 4246–4255.
- (33) Neves, A.; de Brito, M. A.; Vencato, I.; Drago, V.; Griesar, K.; Haase, W. *Inorg. Chem.* **1996**, *35*, 2360–2368.
- (34) Finn, R.; Zubieta, J. *Chem. Commun.* **2000**, 1321–1322.
- (35) Kawafune, I.; Matsubayashi, G.-e. *Bull. Chem. Soc. Jpn.* **1994**, *67*, 694–698.
- (36) Neier, R.; Trojanowski, C.; Mattes, R. *J. Chem. Soc., Dalton Trans.* **1995**, 2521–2528.
- (37) Pohl, M.; Lin, Y.; Weakley, T. J. R.; Nomiya, K.; Kaneko, M.; Weiner, H.; Finke, R. G. *Inorg. Chem.* **1995**, *34*, 767–777.
- (38) Bu, X.; Feng, P.; Stucky, G. D. *J. Chem. Soc., Chem. Commun.* **1995**, 1337–1338.
- (39) Soghomonian, V.; Chen, Q.; Haushalter, R. C.; O'Connor, C. J.; Tao, C.; Zubieta, J. *Inorg. Chem.* **1995**, *34*, 3509–3519.
- (40) Zhang, Y.; Clearfield, A.; Haushalter, R. C. *Chem. Mater.* **1995**, *7*, 1221–1225.
- (41) Cargill Thompson, A. M. W.; Bardwell, D. A.; Jeffery, J. C.; Ward, M. D. *Inorg. Chim. Acta* **1998**, *267*, 239–247.
- (42) Raidt, M.; Neuburger, M.; Kaden, T. A. *Dalton Trans.* **2003**, 1292–1298.
- (43) Tobey, S. L.; Anslyn, E. V. *J. Am. Chem. Soc.* **2003**, *125*, 14807–14815.
- (44) Tobey, S. L.; Anslyn, E. V. *Org. Lett.* **2003**, *5*, 2029–2031.
- (45) Tobey, S. L.; Jones, B. D.; Anslyn, E. V. *J. Am. Chem. Soc.* **2003**, *125*, 4026–4027.
- (46) Zhang, T.; Anslyn, E. V. *Tetrahedron* **2004**, *60*, 11117–11124.
- (47) Wall, M.; Hynes, R. C.; Chin, J. *Angew. Chem., Int. Ed. Eng.* **1993**, *32*, 1633–1635.
- (48) Moreno, Y.; Vega, A.; Ushak, S.; Baggio, R.; Pena, O.; Le Fur, E.; Pivan, J.-Y.; Spodine, E. *J. Mat. Chem.* **2003**, *13*, 2381–2387.
- (49) Phuengphai, P.; Youngme, S.; Pakawatchai, C.; van Albada, G. A.; Quesada, M.; Reedijk, J. *Inorg. Chem. Commun.* **2006**, *9*, 147–151.
- (50) Fernández, I.; Ruiz, R.; Faus, J.; Julve, M.; Lloret, F.; Cano, J.; Ottenwaelde, X.; Journaux, Y.; Muñoz, M. C. *Angew. Chem., Int. Ed.* **2001**, *40*, 3039–3042.
- (51) Yuste, C.; Ferrando-Soria, J.; Cangussu, D.; Fabelo, O.; Ruiz-Pérez, C.; Marino, N.; De Munno, G.; Střiba, S.-E.; Ruiz-García, R.; Cano, J.; Lloret, F.; Julve, M. *Inorg. Chim. Acta* **2010**, *363*, 1984–1994.
- (52) Pardo, E.; Ferrando-Soria, J.; Dul, M.-C.; Lescouëzec, R.; Journaux, Y.; Ruiz-García, R.; Cano, J.; Julve, M.; Lloret, F.; Cañadillas-Delgado, L.; Pasán, J.; Ruiz-Pérez, C. *Chem.—Eur. J.* **2010**, *16*, 12838–12851.

(53) Hatfield, W. E.; Estes, W. E.; Marsh, W. E.; Pickens, M. W.; ter Haar, L. W.; Weller, R. R. In *Extended Linear Chain Compounds*; Miller, J. S., Ed.; Plenum: New York, 1983; Vol. 3, p 43.

(54) Cano, J. *VPMAG package*; University of Valencia: Valencia, Spain, 2003.

(55) Doyle, R. P.; Bauer, T.; Julve, M.; Lloret, F.; Cano, J.; Nieuwenhuyzen, M.; Kruger, P. E. *Dalton Trans.* **2007**, 5140–5147.

(56) Earnshaw, A. *Introduction to Magnetochemistry*; Academic Press: London, U.K., 1968.

(57) *SHELXTL NT*, 6.12; Bruker AXS, Inc.: Madison, WI, 2002.

(58) Sheldrick, G. M. *SHELX-97*; Universität Göttingen: Göttingen, Germany, 1997.